Cytotechnology **45:** 125–140, 2004.

Three-dimensional co-culture of hepatocytes and stellate cells

Susan Fugett Abu-Absi[1], Linda K. Hansen[2] and Wei-Shou Hu[1,*]
[1]*Departments of Chemical Engineering and Materials Science, University of Minnesota Minneapolis, MN 55455-0132 USA;* [2]*Laboratory Medicine and Pathology, University of Minnesota Minneapolis, MN 55455-0132 USA; (*Author for correspondence; e-mail: acre@cems.umn.edu; phone: +1-612-626-7630; fax: +1-612-626-7246)*

Received 8 April 2004; accepted in revised form 21 December 2004

Key words: 3-dimentional culture, Co-culture, Hepatocytes, Stellate cell

Abstract

Hepatocytes self-assemble in culture to form compacted spherical aggregates, or spheroids, that mimic the structure of the liver by forming tight junctions and bile canalicular channels. Hepatocyte spheroids thus resemble the liver to a great extent. However, liver tissue contains other cell types and has bile ducts and sinusoids formed by endothelial cells. Reproducing 3-D co-culture *in vitro* could provide a means to develop a more complex tissue-like structure. Stellate cells participate in revascularization after liver injury by excreting between hepatocytes a laminin trail that endothelial cells follow to form sinusoids. In this study we investigated co-culture of rat hepatocytes and a rat hepatic stellate cell line, HSC-T6. HSC-T6, which does not grow in serum-free spheroid medium, was able to grow under co-culture conditions. Using a three-dimensional cell tracking technique, the interactions of HSC-T6 and hepatocyte spheroids were visualized. The two cell types formed heterospheroids in culture, and HSC-T6 cell invasion into hepatocyte spheroids and subsequent retraction was observed. RT-PCR revealed that albumin and cytochrome P450 2B1/2 expression were better maintained in co-culture conditions. These three-dimensional heterospheroids provide an attractive system for *in vitro* studies of hepatocyte-stellate cell interactions.

Introduction

Primary hepatocytes cultured on moderately adhesive surfaces or in suspension aggregate to form multicellular spheroids (Landry et al. 1985; Koide et al. 1990; Peshwa et al. 1994; Wu et al. 1996). The spheroids sustain excellent viability for extended culture periods and maintain high levels of many liver-specific functions including albumin production, urea synthesis, and cytochrome P450 and glucuronidation activity (Koide et al. 1990; Tong et al. 1990; Lazar et al. 1995; Wu et al. 1996; Wu et al. 1999). Hepatocyte spheroids share many similarities with the native liver, including tight junctions and bile canalicular channels (Asano et al. 1989; Koide et al. 1990; Peshwa et al. 1996; Wu et al. 1996; Abu-Absi et al. 2002), and therefore are a unique and useful model of *in vitro* liver tissue assembly. The spontaneous reorganization of the hepatocytes and the resulting structural similarities between spheroids and liver tissue are intriguing. In the course of self assembly, spheroids develop polarized membrane structure and interconnected bile canalicular channels in which bile acid accumulates (Abu-Absi et al. 2002). The major limitation of spheroids as a model of liver tissue is that they lack other cell types present in the native liver, including those making up the

sinusoids and bile ducts. It is therefore desirable to study the interactions of other liver cell types and hepatocyte spheroids.

Culturing a mixture of cell types has long been considered as a means to prolong the viability and activity of differentiated cells, eliciting responses in cellular behavior absent when the cell types are sequestered. Many co-cultivation studies with hepatocytes have been conducted with liver nonparenchymal cells, fibroblasts, and several immortalized cell lines (Balis et al. 1999). In many cases, the hepatocytes retain the cuboidal shape, granular cytoplasm, and bile canalicular structures that are hallmarks of their organization *in vivo*, but are often lost in traditional monolayer culture (Rojkind et al. 1995; Bhandari et al. 2001). Survival is substantially increased in co-culture conditions, with hepatocyte function detectable to 40–70 days (Guguen-Guillouzo et al. 1983; Gressner et al. 1992). Enhanced albumin secretion (Guguen-Guillouzo et al. 1983; Agius 1988), extracellular matrix production (Guguen-Guillouzo et al. 1983), and tyrosine aminotransferase induction (Yagi et al. 1995) have been observed in co-cultures with nonparenchymal liver cells. Biotransformation activities are also maintained in co-culture. Studies with biliary epithelial cells revealed maintenance of total cytochrome P450 levels out to 10 days, whereas levels in hepatocyte control cultures rapidly decreased (Begue et al. 1984). Culturing hepatocytes with epithelial-like cell lines prolonged the activity of aryl hydrocarbon hydroxylase and certain cytochrome P450 enzymes (Donato et al. 1991). A stabilization in glutathione S-transferase and a slight increase in the activity of UDP-glucuronyltransferase in hepatocyte co-cultures have also been shown (Donato et al. 1991).

Mesenchymal-epithelial cell interactions are important to liver development, as the mesenchyme is involved in the initiation of hepatocyte differentiation (Zaret 2000). Published co-culture studies with mesenchymal stellate cells and hepatocytes have shown increases in cytochrome P450 activity (Okamoto et al. 1998) and prolonged maintenance of hepatocyte function (Rojkind et al. 1995). In addition, stellate cells are implicated in vascularization during liver regeneration (Martinez-Hernandez and Amenta 1995). After liver injury or partial hepatectomy, hepatocytes divide, resulting in a small cluster of hepatocytes with no blood supply. Stellate cells invade the clusters, separating hepatocytes by extending finger-like processes between them and laying down laminin (Martinez-Hernandez and Amenta 1995). Endothelial cells then begin to proliferate and migrate along the laminin trail to form sinusoids between the hepatocytes, thus restoring the plate structure of the liver acinus. Since stellate cells play such an important role in restoring normal architecture to the liver, it is of interest to study their behavior in culture. The spheroid is a suitable *in vitro* model of the hepatocyte cluster described above, and co-culture with stellate cells might provide a means to incorporate endothelial cells and potentially endothelial-cell lined ducts in a structured fashion without artificial scaffolding.

To investigate interaction between hepatocytes and stellate cells, a co-culture method was developed using primary rat hepatocytes and a rat hepatic stellate cell line, HSC-T6 (Vogel et al. 2000). Initial studies to develop the co-culture method were performed with a stellate cell line due to ease of maintenance and readily available cells. In addition, the HSC-T6 is an activated stellate cell line with a similar phenotype to stellate cells participating in liver regeneration, whereas primary stellate cells require time in culture to become activated. The HSC-T6 cells were first characterized by RT-PCR to screen for the expression of known stellate cell markers. Next, liver specific protein and gene expression in co-culture were analyzed. Finally, the distribution of the two cell types in culture was characterized.

Materials and methods

All study protocols were reviewed and approved by the University of Minnesota Research Animal Resources Animal Care Committee and met the institutional and national guidelines for the humane care and use of research animals. All reagents were purchased from Sigma Chemical Company (St. Louis, MO), unless otherwise noted.

Isolation of primary hepatocytes

Rat hepatocytes were harvested from 4–6 week old male Sprague-Dawley rats weighing 200–250 grams by a two-step *in situ* collagenase perfusion technique modified from Seglen (1976) and

described in more detail elsewhere (Abu-Absi et al. 2002). Each harvest routinely yielded hepatocytes with viability greater than 90% based on trypan blue exclusion.

HSC-T6 stellate cell line

The immortalized hepatic stellate cell line HSC-T6 was obtained from Dr. Scott Friedman (Mount Sinai School of Medicine, New York, NY). The cell line was originally developed from 15 day activated primary rat stellate cells by transformation with a plasmid encoding the SV40 large T antigen (Vogel et al. 2000). HSC-T6 cells were cultured in DMEM/F12 medium supplemented with 4 mM L-glutamine, 100 U/ml penicillin and 100 μg/ml streptomycin (all from Life Technologies, Rockville, MD). Originally maintained in 10% FBS, the cells were weaned to 2% FBS by decreasing the serum concentration gradually over the course of a week. Cells were passaged (1:20) every 3 days by trypsinization with a 0.05% trypsin solution. Cultures were maintained in a 37 °C, 5% CO_2, humidified incubator.

Culture setup

Spheroid formation in stationary culture was achieved by culturing hepatocytes on 35-mm or 60-mm Falcon Primaria dishes (Becton Dickinson, Franklin Lakes, MJ) at approximately 42,000 cells/cm^2, as previously described (Hansen et al. 1998). Hepatocytes were cultured in spheroid medium consisting of a basal Williams' medium E supplemented with 0.2 U/ml insulin (Eli Lilly, Indianapolis, IN), 100 U/ml penicillin, 100 μg/ml streptomycin, 2.0 mM L-glutamine, 50 ng/ml mouse epidermal growth factor, 50 μg/ml linoleic acid-albumin (Sigma L-8384), 15.0 mM *N*-2-hydroxyethylpiperazine-N′-2-ethane sulfonic acid (HEPES, Life Technologies), 0.1 μM $CuSO_4 \cdot 5H_2O$, 30 nM Na_2SeO_3, and 50 pM $ZnSO_4 \cdot 7H_2O$. HSC-T6 cells were subsequently added to the hepatocyte culture at the times indicated for each experiment (typically 8 h after seeding or after the formation of spheroids) by trypsinizing one or more T-flasks. Once the cells had detached from the flask, an equal volume of Williams' E medium containing 1 mg/ml soybean trypsin inhibitor was added to quench the activity of the trypsin. The cells were then pelleted at $90 \times g$, and resuspended in fresh spheroid medium. After determining the cell concentration by counting with a hemacytometer, HSC-T6 cells were added to the hepatocytes in a ratio of 1:10.

Dual dye labeling

Hepatocytes and HSC-T6 cells were stained with vital membrane dyes for visualization. Stock solutions of 10 mg/ml 1,1′-dioctadecyl-3,3,3′,3′-tetramethylindocarbocyanine perchlorate (DiI) and 0.5 mg/ml 3,3′-dioctadecyloxacarbocyanine perchlorate (DiO), (Molecular Probes, Eugene, OR), were prepared in a solution of one part dimethyl sulfoxide (DMSO) and nine parts ethanol. Prior to use, DiI and DiO stock solutions were sonicated to completely dissolve any particulates. For labeling, DiI or DiO stock solutions were diluted in medium to final concentrations of 50 mg/ml and 25 mg/ml for DiI and DiO, respectively. Cells were then mixed with the dye solution and incubated for 15 min at 37 °C to allow the dye to incorporate into the plasma membrane. The cells were then washed three times and counted. Hepatocytes were first labeled with DiI and cultured to form spheroids as described above. HSC-T6 cells were labeled with DiO and added to the dishes containing DiI-stained hepatocytes at a ratio of 1:10 HSC-T6:hepatoctyes at the indicated time. Cultures were maintained in a 37 °C, 5% CO_2, humidified incubator. Medium was changed at or before 24 h and every 2–3 days thereafter.

Time-lapse confocal microscopy

For time-lapse studies, hepatocytes were cultured in a modified Williams' medium E in which the sodium bicarbonate concentration was reduced to 2 mM to facilitate experimentation in ambient air. To balance osmolarity and replace sodium ions normally contributed by the sodium bicarbonate, 1.39 g/l sodium chloride was added. This low bicarbonate Williams' E medium was then supplemented as above. Cultures were maintained at 37 °C in ambient air without CO_2 addition.

The apparatus for time-lapse microscopy was comprised of an HCC-100A temperature

controller (Dagan Corporation, Minneapolis, MN) positioned on the stage of an inverted Nikon Diaphot epifluorescence microscope linked to an argon laser confocal scanning system (Multiprobe 2001, Molecular Dynamics, Mountain View, CA). The thermal stage consisted of an aluminum block heated and cooled through Peltier elements, a seat to hold a 35 mm culture dish, and thermistors to monitor both the temperature of the block and the temperature of the solution in the petri dish (bath). Culture dishes were filled completely with medium and sealed using stopcock grease to prevent evaporation. A small air bubble was left in the dish to supply oxygen and a hole drilled through the lid provided access for the bath temperature thermistor. The bath temperature in the dish was maintained at 37 °C using a dual integrative feedback loop between the thermistors from the block and bath and the stage was cooled by cold tap water delivered through silicon tubing. The thermal stage was set up and allowed to equilibrate to 37 °C using a trainer dish containing water. Once the temperature of the block was optimal for temperature control at 37 °C, the trainer dish was replaced by the petri dish containing cells.

Time-lapse series scans were taken with the confocal laser scanning microscope under control of an Iris Indigo Silicon Graphics workstation and ImageSpace software version 3.2 (Molecular Dynamics). A 10x/0.45 objective lens was used for all studies and laser power was constrained to the lowest possible stable output, typically 7–7.5 mW. Fluorophores were excited with the 488 nm laser line and resulting emitted light was passed through a 100 μm pinhole aperture followed by a 595 nm beam splitter. Light of wavelength greater than 595 nm was directed through a 600 nm extended pass filter and Dil fluorescence was detected with a photomultiplier tube. Light emitted below 595 nm was directed through a 530 ± 15 nm baud pass filter and DiO fluorescence was detected with a second photomultiplier tube. Series scans of the same field of view were taken every hour using the time-lapse function in the ImageSpace program and images of the two channels were stored separately. Images 512×512 pixels in size were collected for each section scan, each pixel corresponding to 1 μm, and series scans were taken at a step size of 1–2 μm. Images were stored in pseudo-color using a 256-scale color map.

Three-dimensional reconstruction of time-lapse data

Reconstruction of three-dimensional images was accomplished using IBM Visualization Data Explorer (DX) (Version 3.1.4, IBM Corp. Yorktown Heights, NY) on an IBM SP2 at the University of Minnesota Supercomputing Institute. Raw data taken with the ImageSpace software were stored as 512×512 matrices of pixel intensities ranging from 0–255. The data were first binarized using a simple Fortran code to set the values of all pixels above a chosen threshold to 255 and all values below to 0. Thresholds were chosen based on visual examination of the raw data to produce realistic three-dimensional images. Next, the binarized matrices from serial scans were stacked into an array and imported into the DX program. Red (for DiI-stained cells) and green (for DiO-stained cells) datasets were processed separately, and shaded isosurfaces were used to connect pixels of intensity 255. To achieve a look-through effect, the red and green images were overlaid and blended. Red isosurfaces were transparent so that green cells could be visualized at all times.

Measurement of albumin and urea concentration

Rat albumin concentrations in the culture medium were determined by a competitive enzyme-linked immunoassay (ELISA) as described previously (Tzanakakis et al. 2001). Urea concentrations were determined by a Urea Nitrogen Diagnostic Kit (Sigma, procedure No. 640) based on a technique developed by Fawcett and Scott (1960) and simplified by Chaney and Marback (1962) following the manufacturer's instructions. Statistical analysis was carried out using the Analysis ToolPak of Microsoft Excel 2000 (Microsoft Corp., Redmond, WA). Comparisons were performed using a two-tailed homoscedastic Student's T-test.

Determination of viability with confocal microscopy

Viability was assessed with fluorescein diacetate/ethidium bromide (FDA/EB) staining as previously described (Tzanakakis et al. 2001). FDA is cleaved by esterases in live cells producing the fluorescent molecule fluorescein, while ethidium bromide penetrates through the membrane of dead

cells binding to the nuclear DNA. Staining was visualized with confocal microscopy at an excitation of 488 nm, collecting light above 600 nm (EB) and at 530 ± 15 nm (fluorescein) using an aperture of 50–100 μm.

Reverse transcriptase polymerase chain reaction

Cells were scraped from the dishes and collected by centrifugation at $50 \times g$. The cell pellet was immediately frozen in cryo vials in liquid nitrogen in a minimal amount of medium. Total RNA was isolated by two extractions wih TriZol® reagent (Life Technologies) following the manufacturer's instructions. Purity and integrity of RNA samples were verified by electrophoresis on a 1.4% agarose gel in 10 mM sodium phosphate buffer, pH 6.8. Genomic DNA contamination was eliminated from the RNA by treatment with DNase I (Ambion, Austin, TX). Total RNA was then extracted using phenol:chloroform. Briefly, an equal volume of acid phenol:chloroform mixture, pH 4.5 (Ambion) was added to the sample and centrifuged at $12{,}000 \times g$ for 10 min at 4 °C. The RNA, which segregated to the aqueous phase, was transferred into a fresh tube and was precipitated by the addition of 0.3 M sodium acetate and 70% ethanol and overnight incubation at −80 °C. RNA was collected by centrifugation at $12{,}000 \times g$ for 1 h. The resulting pellet was washed with 75% ethanol and dried. The RNA was resuspended to a final concentration of 1 μg/μl in RNAse-free water and stored at −80 °C until further use.

RT-PCR was carried out with the SUPERSCRIPT™ One-Step RT-PCR system (Life Technologies). cDNA synthesis and PCR were performed in a single tube using gene-specific primers and target RNA. A TouchGene thermal cycler (Techne, Inc., Princeton, NJ) was used to carry out the RT-PCR. cDNA synthesis was achieved at 45 °C for 45 min. After a 2 min predenaturation cycle at 94 °C, PCR amplification was performed by cycles of 15 s denaturing at 94 °C, 30 s annealing at 56 °C, and extension for 1 min at 72 °C. Cycle optimization was performed on each set of primers to ensure that single products were produced in the linear range of amplification. Sequence-specific primers were found in the literature or derived from rat sequences available at GenBank (http://www.ncbi.nlm.nih.gov/) using Primer3 software (http://www-genome.wi.mit.edu/cgi-bin/primer/primer3_www.cgi) and synthesized by Integrated DNA Technologies, Inc. (Coralville, IA). Table 1 lists the sequences of the primers, the number of PCR cycles performed with each primer pair, and the GenBank accession number and/or reference. PCR products were run on a 2% agarose gel in TAE buffer (Sambrook et al. 1989) and visualized with ethidium bromide. Gels were imaged on a transilluminator equipped with a digital camera. Quantitative analysis of the images was performed using Kodak 1D Digital Science Software. Each product was quantified by intensity integration in a rectangular region demarcating the band. Background signals were subtracted before integration. Normalization of the data was accomplished by calculating the ratio of the integrated intensity of the band relative to the integrated intensity of the E-cadherin product band.

Results

Characterization of the stellate cell line

The rat hepatic stellate cell line, HSC-T6, was used in the co-culture experiments. This cell line was developed by transforming primary rat stellate cells after they had been activated by culture in plastic dishes (Vogel et al. 2000). The activated phenotype of stellate cells is displayed during times of wound healing *in vivo*. It is characterized by increased extracellular matrix production, changes in growth factor secretion, enhanced proliferation and a fibroblastic appearance (Friedman 1996). Previous studies with HSC-T6 established that they display a number of activated stellate cell markers (Ankoma-Sey et al. 2000; Vogel et al. 2000). In culture, they proliferate rapidly and exhibit a fibroblast-like morphology (Figure la). They express several cytoskeletal proteins typical of activated stellate cells including smooth muscle α-actin (α-SMA), vimentin, glial fibrillary acidic protein and desmin, as shown by immunocytochemical detection (Vogel et al. 2000). They also express the transcripts of all six retinoid nuclear receptors and cellular retinal-binding protein type I, similarly to primary stellate cells (Vogel et al. 2000). We further characterized these

Table 1. Primers used for RT-PCR studies.

Gene	Cycles	Primer sequences	Product size	Accession #	Reference
Albumin	30	F: GAG ATT CCG AGC AGG ACA AG R: CAA AGC AGG GTC TCC TGA AG	504	X76456	
α-SMA	40	F: GAG CAT CCG ACC TTG CTA AC R: TGA AAG ATG OCT GGA AGA GG	502	X06801	
Collagen I	38	F: CTG CTG GAG AAC CTG GAA AG R: AGA ACC ATC AGC ACC TTT GG	506	Z78279	
Collagen III	38	F: CTT GGA ATT GCA GGG CTA AC R: GGG AAT CCT CGA TGT CCT TT	497	X70369	
Connexin 43	40	F: CIT CTG GAC AAG GTC CAA GC R: ACC ACT GGA TGA GCA GGA AG	496	NMOl2567	
CPS-I	30	F: GGA TGT TGT TGC CAA ACC IT R: CAT CTG CTG ACA TCC TCC AA	507	Z275 13	
Cyclophilin	20	F: CTT CGA CAT CAC GGC TGA TGG R: CAG GAC CTG TAT GCT TCA GG	265		a
CYP2Bl/2	38	F: GAG TTC TTC TCT GGG TTC CTG R: ACT GTG GGT CAT GGA GAG CTG	549		a
CYP3A2	38	F: GCA TAA GCA CCG AGT GGA TT R: CAA TGC TTC CCT TGT TCT CC	494	U09742	
E-Cadherin	30	F: GCT GGA GAC CAG TTT TCT CG R: TCT GGC CTG TTG TCA TTC TG	504	NM031334	
Laminin	40	F: TCG TTG TCC ATG TCA AGA CC R: GTG TAC CCA GGA GGA GAA TCT G	298	S72407	b

a – (Morris and Davila 1996)
b – (Maher and Tzagarakis 1994)

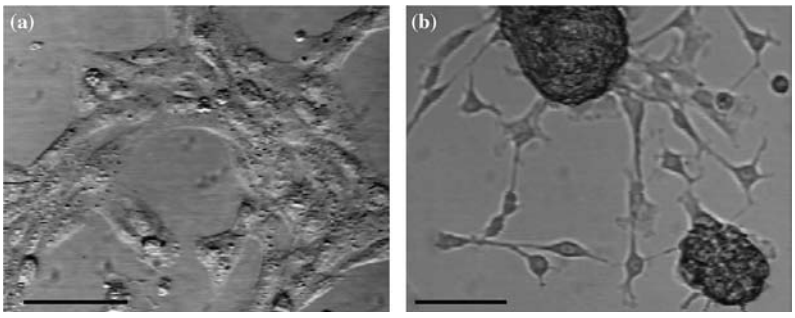

Figure 1. Morphology of HSC-T6 in maintenance culture and co-culture after 6 days. HSC-T6 cultured (a) alone on tissue culture plastic in 2% FBS and (b) in serum-free medium on Primaria dishes with hepatocytes exhibited differences in morphology. Scale bars indicate 50 μm.

cells to confirm the expression of mRNA encoding α- SMA, connexin 43 (a gap junction protein known to be produced in stellate cells (Greenwel et al. 1993)), the stellate cell-derived M subunit of laminin (Maher and Tzagarakis 1994), and collagen types I and III (results not shown). In addition, RT-PCR revealed that the HSC-T6 cells did not express albumin, carbamoylphosphate synthetase–I (CPS-I), cytochrome P450 2B1/2 (CYP2B1/2), cytochrome P450 3A2 (CYP3A2), or E-cadherin (results not shown).

Morphological observations during co-culture with HSC-T6

HSC-T6 cells were originally cultured in medium supplemented with 10% FBS, in which they grow rapidly. For the co-culture studies, it was necessary to culture the hepatocyte in serum-free spheroid medium, as spheroid formation is inhibited in the presence of FBS, and cytochrome P450 activities are reduced in the presence of FBS (Hsiao et al. 1999). The possibility of culturing HSC-T6 in the

spheroid medium without serum was explored. Initially, the HSC-T6 cells attached to the dish, but remained slightly more rounded than in maintenance culture with FBS. Figure 2 displays the results of the viability assay on HSC-T6 cells after one day (a–b) and 2 days (c–d) in culture, in which viable cells appear green and the nuclei of dead cells stain red. The panels on the left show fluorescence images, with corresponding transmission images on the right. After a day in culture, the HSC-T6 cells were mostly viable and had formed cord-like structures on the dish. The next day, however, the cells had formed loose aggregates with very poor viability. Staining performed after 3 days revealed even fewer viable cells (not shown). Since HSC-T6 cells do not survive in serum-free spheroid medium, they were cultured over a two week period with successive decreases in FBS concentration upon passaging. The final FBS concentration used for their maintenance was 2%. When HSC-T6 cells were grown in co-culture with hepatocyte in serum-free spheroid medium, however, they not only survived, but maintained the ability to proliferate.

For three-dimensional co-culture studies, hepatocytes were plated in spheroid medium on Primaria dishes. After hepatocyte attachment (~8 h), HSC-T6 cells were added to the culture in a 1:10 ratio of stellate cells: hepatocytes. Hepatocytes initially attached to the culture dish as a monolayer then gradually aggregated to form spheroids. The morphological changes of hepatocytes during spheroid formation have been described previously (Peshwa et al. 1994). During the first few days in culture, it was very difficult to identify the HSC-T6 cells in the midst of the hepatocytes due to their relatively small size (about 10 μm in diameter compared to hepatocytes as large as 20 μm) and their tendency to spread out between hepatocytes. Initially, the HSC-T6 cells preferentially grew around the hepatocytes, but eventually began to spread to bare regions of the dish (Figure 3b). After about 4 days in culture the HSC-T6 cells became more visually distinguishable as they continued to proliferate. Eventually, the HSC-T6 cells formed an outer cell layer around hepatocyte spheroid cores. The HSC-T6 cell layer around the hepatocytes anchored the spheroids to the culture dish. In contrast, spheroids cultured alone released from the dish and were suspended in the medium (Figure 3a). The

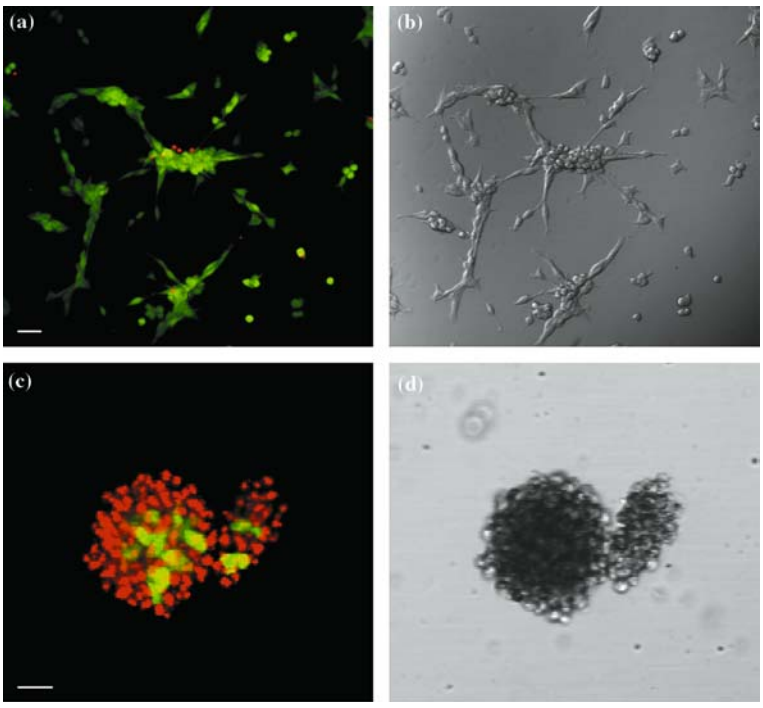

Figure 2. Viability of HSC-T6 cultured alone on Primaria in serum-free spheroid medium. HSC-T6 were transferred into serum-free spheroid medium and cultured on Primaria dishes. Viability stains (a–b) after one day and (c–d) after 2 days in culture. Panels on the left are fluorescence images and corresponding transmission images are shown on the right. Scale bars indicate 20 μm.

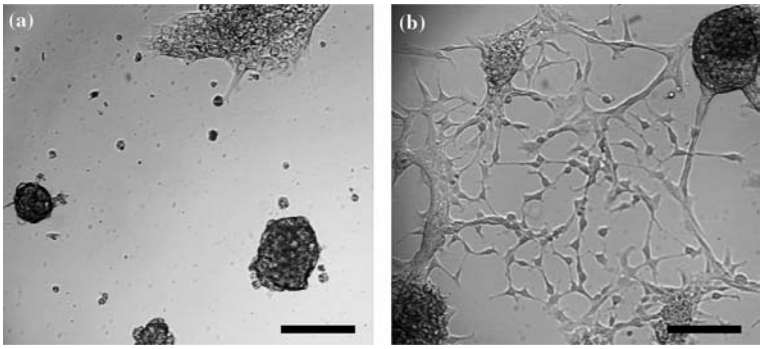

Figure 3. Morphology of homo- and heterospheroids. For control cultures, hepatocytes were cultured alone in serum-free medium to form spheroids. Co-culture dishes were set up by adding HSC-T6 to hepatocytes during the monolayer stage of spheroid formation. (a) Control culture and (b) co-culture after 6 days in culture. Scale bars indicate 100 μm.

continual proliferation of the HSC-T6 cells could become problematic in the later stages of the co-culture. The pH decreased more rapidly due to the extra lactic acid produced by the HSC-T6 cells and nutrients were more quickly consumed than in hepatocyte cultures. To remedy the problem of stellate cell proliferation overtaking the culture, stellate cells were seeded in the co-culture at a low cell density and medium exchanges or additions were performed often.

The HSC-T6 cells underwent a morphological change when cultured in serum-free spheroid medium with hepatocytes. When cultured alone in 2% serum in tissue culture flasks, they appeared very fibroblastic and well-spread, characteristics associated with activated stellate cells (Figure la). However, when co-cultured with the hepatocytes in spheroid medium, they had star-shaped bodies and thin projections (Figure 1b). This star-shaped appearance is typical of quiescent stellate cells *in vivo* (Majno 1979). It is speculated that loss of contact with hepatocytes *in vivo* may lead to stellate cell activation (Friedman 1996; Senoo et al. 1998), which may explain why HSC-T6 cells in co-culture with hepatocytes revert back to a star-shaped morphology.

Effects of co-culture with HSC-T6 on liver-specific protein production

For studies of albumin and urea production, HSC-T6 cells were added to hepatocyte culture as described above and hepatocytes were cultured alone as controls. After 24 h, the medium was aspirated from all the dishes and 2 ml fresh medium added. To replenish nutrients from then on, fresh medium (0.5 ml) was added to the dishes every 2–3 days, but medium was not withdrawn to prevent removal of cells. On days 3, 6, 9, and 14 three dishes per condition were sacrificed and medium was collected for measurements of urea and albumin content. This experiment was repeated with cells from three rats, all with similar results.

Results from a representative experiment are shown in Figure 4. Figure 4a shows urea concentration in the culture. Error bars represent the standard deviation among the three dishes in each sample. The cumulative amount of urea produced was calculated and is shown in Figure 4b. Figure 4c and d show the same results for albumin production. Urea production in the co-cultures was virtually identical to the controls. However, the presence of the HSC-T6 cells had a positive effect on albumin production. By day 9, there was a noticeable difference in albumin concentration, co-culture dishes having more than twice the amount of albumin than controls. The albumin concentration on day 14 was statistically higher in the co-culture dishes, as determined by a Student's T-test ($p < 0.005$). Cumulative production (Figure 4d) shows a plateau of albumin production in the control culture, but a continued rise in production in the co-culture dishes resulting in approximately two times more albumin.

Effects of co-culture with HSC-T6 on liver-specific gene expression

The expression of a number of genes was assessed by RT-PCR in hepatocytes cultured alone on

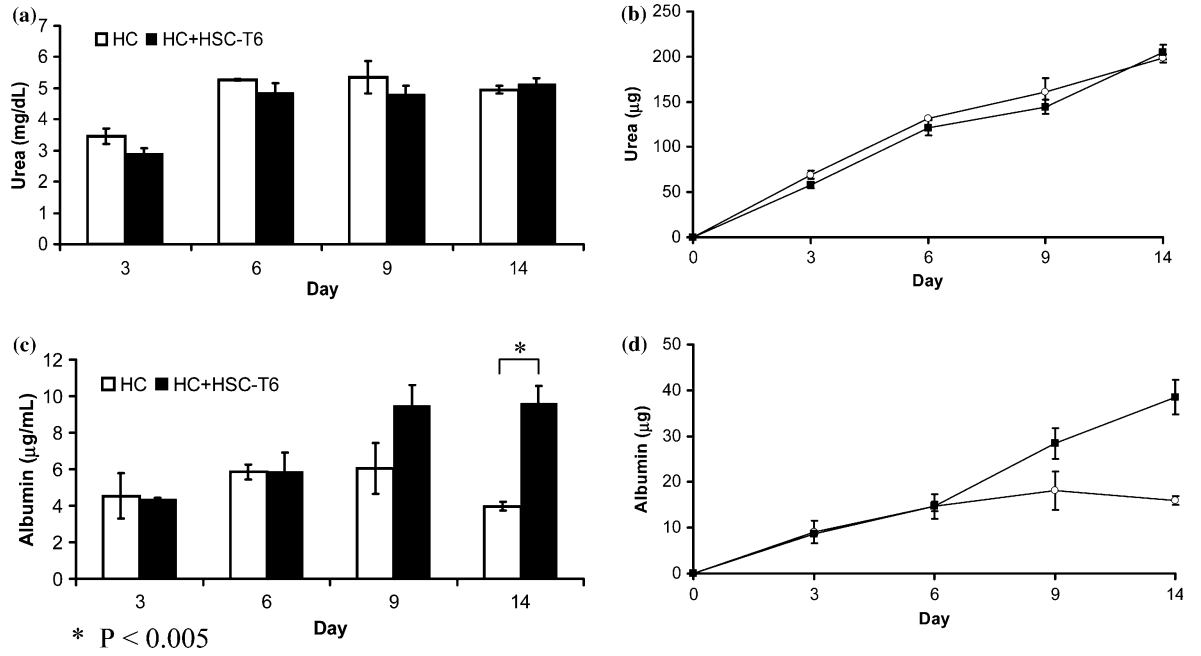

Figure 4. Liver-specific protein production in co-culture. Hepatocytes were cultured on 35-mm Primaria dishes to form spheroids. HSC-T6 cells were added to half of the dishes after hepatocytes had attached (~8 h). On days 3, 6, 9, and 14 three dishes per condition were sacrificed and measurements of urea and albumin concentration were taken. Fresh medium was added to the dishes every 2–3 days to replenish nutrients, but medium was not withdrawn to prevent removal of spheroids. (a) Urea and (c) albumin concentration in control (white bars) and co-cultures (black bars). Error bars indicate standard deviation among the three dishes sampled. Cumulative production of (b) urea and (d) albumin in control cultures (○) and co-cultures (■).

Primaria dishes and those in co-culture with HSC-T6. Hepatocyte number in the culture was constant since they do not proliferate under these conditions, but the HSC-T6 cells proliferated throughout the culture period. Therefore, a method to normalize gene expression based on hepatocyte number was necessary for proper interpretation of the results of RT-PCR. E-cadherin is expressed in hepatocytes but not in the mesenchymal HSC-T6 cells and its expression level throughout spheroid formation is constant (not shown). Therefore the level of E-cadherin mRNA was used as an indicator of hepatocyte cell number. Cyclophilin, a housekeeping gene, was used as a marker of total cell number, since both cell types constitutively express it. Four liver-specific genes were probed. In addition to albumin, carbamoylphosphate synthetase–I (CPS-I, the enzyme that catalyzes the first step of the urea cycle), and cytochrome P450 enzymes 3A2 and 2B1/2 (involved in xenobiotic metabolism) were monitored. Total RNA was collected after 1 and 14 days in culture and RT-PCR was carried out with sequence-specific primers. PCR products were run on a 2% agarose gel and band intensities, visualized by ethidium bromide staining and quantified by image analysis, and were compared to the intensity of the E-cadherin band to normalize for hepatocyte cell number. This was carried out with cells from three separate hepatocyte harvests.

The results of the RT-PCR are shown in Figure 5. Figure 5a shows a representative gel of the PCR products and Figure 5b shows the normalized band intensities on days 1 and 14 from three hepatocyte harvests along with their average. Error bars indicate standard deviation among the three hepatocyte harvests. There is considerable variation from rat to rat, particularly with respect to the albumin mRNA levels, which were very low in the hepatocytes from harvest 1. Statistical analysis of the RT-PCR results is meaningless due to the small sample size and large difference between rats; however, in cells from all three hepatocyte preparations, albumin mRNA levels were higher on day 14 in co-culture, and the normalized albumin band intensities for the co-culture dishes

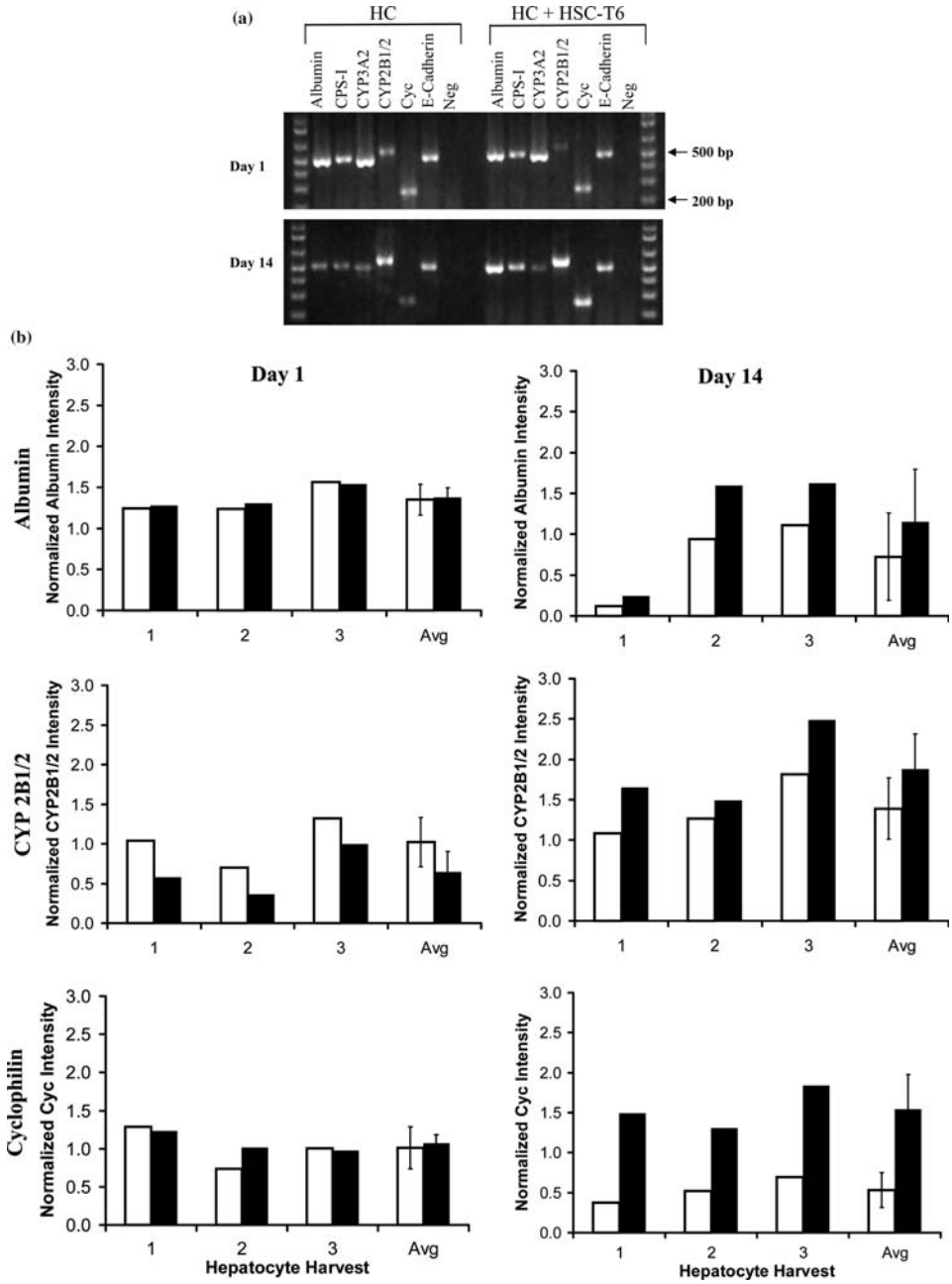

Figure 5. Liver-specific mRNA levels in co-culture. Spheroids were cultured alone and with HSC-T6 on Primaria and total RNA was isolated on days 1 and 14. RT-PCR was used to compare mRNA levels of albumin, CPS-I, CYP3A2, CYP2B1/2, cyclophilin (eye), and and E-cadherin. (a) Representative agarose gel of PCR products. Ethidium bromide intensity from each band was normalized by the intensity of the E-cadherin band. E-cadherin is expressed by hepatocytes and not HSC-T6 cells and used to normalize based on hepatocyte content. Negative controls were included by running the RT-PCR reaction without primers. (b) Average intensities from three separate harvests for albumin, CYP2B1/2, and cyclophilin for control cultures (white bars) and co-cultures (black bars) on days 1 and 14. Error bars indicate standard deviation among the three hepatocyte preparations.

were about 1.7 times higher than control. Likewise, CYP2Bl/2, for which the transcript was initially lower in the co-cultured cells, was about 1.4 times higher in all three cases by day 14. No marked variation between control cultures and co-cultures were found for CPS-I or CYP3A2. Since

both cell types express cyclophilin and the HSC-T6 divide under culture conditions, it was found at higher levels in the co-culture dishes on day 14, as expected (Figure 5b).

Cell distribution and interaction during co-culture with HSC-T6

Hepatocytes were labeled with the red membrane dye DiI and plated on Primaria dishes to allow for spheroid formation. DiO-labeled HSC-T6 cells (green) were added to the cultures 8 hours later. At that time point hepatocytes were still largely attached and spread on the surface (Figure 6a). HSC-T6 cells (green) preferentially localized near hepatocytes and spread out on the interior and periphery of the hepatocyte patches. A control experiment was performed (not shown) whereby hepatocytes were allowed to attach to only one half of a Primaria dish. The HSC-T6 cells, upon inoculation to the culture, attached to hepatocytes in the dish and not the exposed surface. In most cases they attached to the surface attached hepatocytes, but were also found as floating clusters or attached to floating hepatocytes. Although HSC-T6 cells, when cultured alone, are capable of attaching to Primaria (Figure 2), they prefer to attach to the hepatocytes. The patches of hepatocyte and HSC-T6 cells agglomerated and proceeded to form heterospheroids. In the heterospheroids hepatocytes were typically seen in the interior and HSC-T6 around the periphery. A similar distribution of cells was observed after the addition of HSC-T6 cells to mature spheroids (Figure 6b). HSC-T6 cells again remained mostly separate from hepatocytes, and some homospheroids, comprised of mostly one cell type, were found.

To observe the physical interactions between the hepatocytes and HSC-T6 cells, time-course and time-lapse investigations were carried out by dual labeling and confocal microscopy. Once DiI labeled spheroids had formed, HSC-T6 cells labeled with DiO were added to the culture and adhered to the surface of the spheroids. After 10 hours, time-lapse scans were initiated with the confocal microscope. A 20 μm-thick cross section through the spheroid was monitored to track the movement of the green HSC-T6 cells on the periphery.

Figure 7 displays the time-lapse micrographs. Grayscale images show raw data of the position of the green HSC-T6 cells. Corresponding three-dimensional representations of the 20 μm-thick slab through the spheroid are shown below. Initially, the HSC-T6 cells attached to the surface of the spheroid. However, about 3 h after the time-lapse was initiated, HSC-T6 cell (1) invaded the spheroid (Figure 7a). That cell and possibly a few others then extended thin processes between hepatocytes a few layers deep into the spheroid (Figure 7b). Vertical scans throughout the spheroid verified that the HSC-T6 cells had actually penetrated the spheroid (not shown). These cells remained in the midst of the hepatocytes for some time, but eventually retracted (Figure 7d–e) and resumed their original position on the periphery of the spheroid (Figure 7f). Throughout this time-

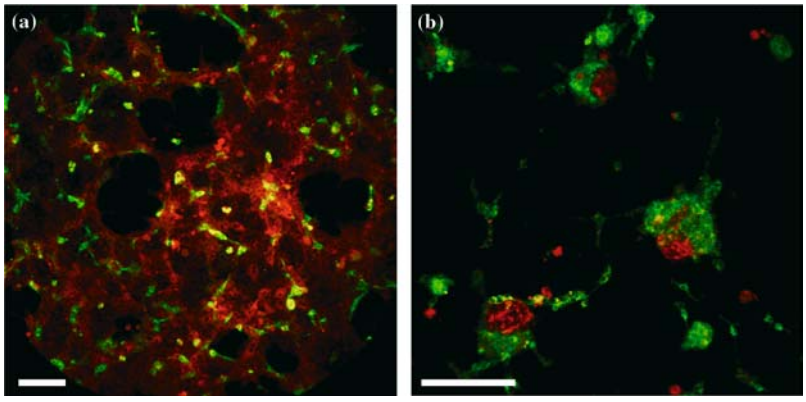

Figure 6. Cell distribution in co-culture. Hepatocytes were labeled with DiI (red) and plated for spheroid formation on Primaria dishes. HSC-T6 were labeled with DiO (green) and added to (a) hepatocytes in the monolayer stage of spheroid formation or (b) to mature spheroids. Images were taken at (a) 2 days and (b) 4 days. Scale bars indicate 20 μm.

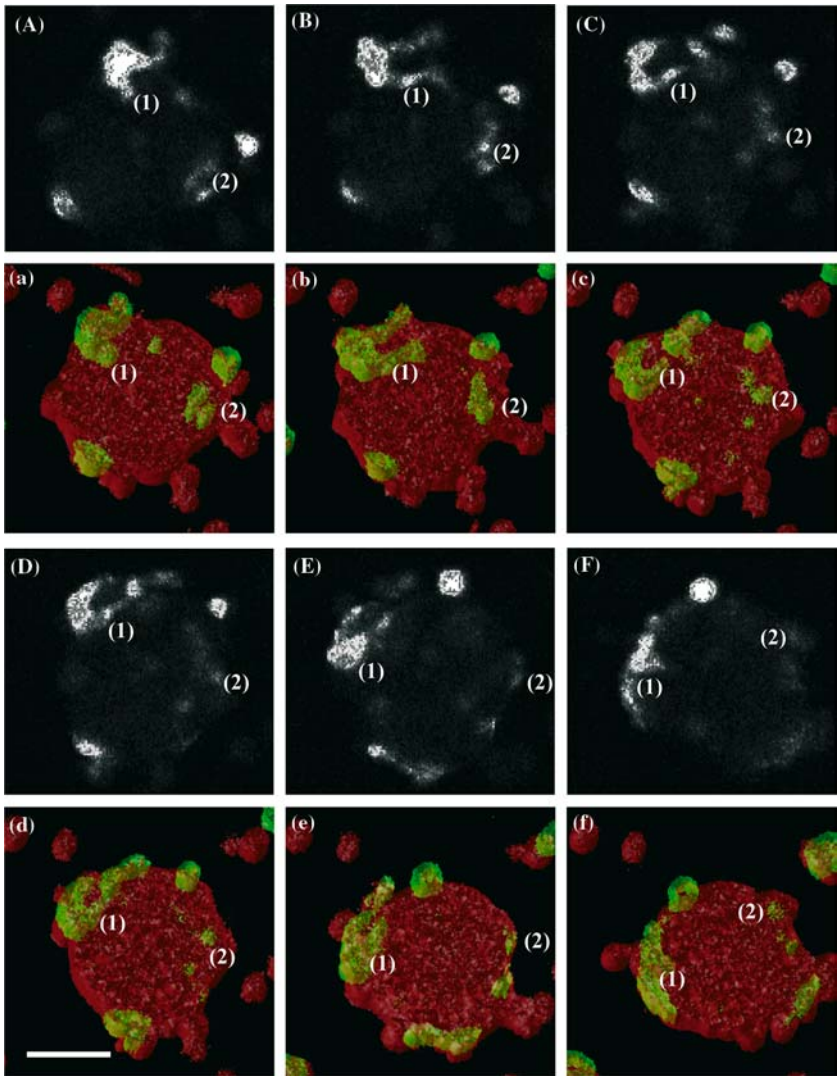

Figure 7. Cell dynamics during time-lapse study of co-culture. Grayscale images of the HSC-T6 cells (capital letters) and corresponding 3-D reconstructions (lowercase letters) at (a) 3, (b) 5, (c) 7, (d) 8, (e) 13, and (f) 17 h after initiation of the confocal scans. Two HSC-T6 cells are labeled (1) and (2) and tracked throughout the images. Scale bar indicates 50 μm.

lapse experiment, the microscope was adjusted to keep cell (1) in focus. A similar invasion/retraction was also observed for another group of cells (2). Initially, their position was inside the spheroid (Figure 7a). However, they drifted out of the plane of focus (Figure 7c–d) and reemerged as separate flattened cells on the surface of the spheroid (Figure 7e). Time-course studies revealed very similar results (not shown). Initially the HSC-T6 cells were distributed only on the perimeter of the hepatocyte spheroids, but after a day or so a few HSC-T6 cells were found inside the spheroids. However, the inside of the spheroids were never completely occupied by a large number of stellate cells. By the end of the time course experiments, the HSC-T6 cells were once again found primarily on the surface of the spheroids.

Discussion

Stellate cells interact both physically and chemically with hepatocytes *in vivo*. They lie in the perisinusoidal space in the liver and have spine-like

processes in direct contact with the microvilli on the basal domain of the hepatocytes. They also produce hepatocyte growth factor, transforming growth factor α, and EGF, which are all potent mitogens for hepatocytes (Schirmacher et al. 1992; Friedman 1996). In return, hepatocytes influence stellate cells by expressing insulin-like growth factor I that activates stellate cell proliferation *in vitro* (Gressner et al. 1995). Our results are consistent with many other published co-culture findings. Co-culture with the HSC-T6 cells generates a moderate enhancement in albumin production by the hepatocyte spheroids. Albumin production in co-culture was sustained to at least 14 days, whereas it reached a plateau by about 7 days in control cultures. It is common for the advantages of co-culture to develop after 7 days in culture (Guguen-Guillouzo et al. 1983; Bhatia et al. 1998). Likewise, hepatocytes in monolayer co-cultures with stellate cell lines from cirrhotic liver expressed high levels of liver-specific mRNA and secreted liver-specific proteins for up to 2 weeks (Rojkind et al. 1995). In our study the expression of albumin and CYP2B1/2 mRNA was higher in the co-cultured hepatocytes by 14 days, while the mRNA of the other genes probed was present in similar quantities and no difference in ureagenesis was observed between co-cultures and controls. Higher cytochrome P450-mediated lidocaine metabolism to MEGX with no enhancement in ureagenesis was also observed in a previous co-culture study with human hepatocytes and a human stellate cell line, L190 (Okamoto et al. 1998). MEGX production is mediated by CYP3A4 in humans and lA2, 2Cll, 2Bl, and 3A2 in the rat (Imaoka et al. 1990). Since rat stellate cells themselves express CYP3A2, this effect may not have been solely due to increased hepatocyte activity.

HSC-T6 cells could not sustain viability when cultured in serum-free medium. However, they were able to grow under co-culture conditions. A similar increase in 3T3 cell survival with hepatocytes was reported by Bhandari and colleagues (Bhandari et al. 2001). In addition, it appears that the HSC-T6 cells in co-culture adopt a more quiescent morphology. A previous study reported a decreased expression of α-SMA in stellate cells cultured in hepatocyte conditioned medium, also indicating a decrease in stellate cell activation (Gressner et al. 1992). However, further studies of potential gene expression changes are necessary to completely elucidate the controlling factor(s) in our system and whether the HSC-T6 cells are actually undergoing a reversion to the quiescent phenotype in the presence of the hepatocytes.

A few groups have also investigated the effect of culturing hepatocytes with other cells in a three-dimensional configuration. Michalopoulos et al. developed a culture system of hepatocytes and nonparenchymal liver cells on collagen-coated microbeads in roller bottles (Michalopoulos et al. 1999). The cultures were subsequently placed in Matrigel and cultured further. The resulting structures mimicked the liver as hepatocytes arranged themselves into plates with bile canalicular networks. In addition, vascular structures of fenestrated endothelium were developed and desmin-positive cells surrounded the hepatocytes. Heterospheroids have been formed previously by culturing parenchymal and nonparenchymal cells as a monolayer on a thermoresponsive polymer that dissolves at temperatures below 30 °C (Ueno et al. 1992). Upon lowering the temperature of the culture to dissolve the polymer substratum, the monolayer folds up upon itself to form a heterospheroid. The nonparenchymal cells in these heterospheroids segregated to the periphery of the spheroids similarly to what we observed in our heterospheroids, but no studies were performed to elucidate the mechanism of the segregation or effects of the heterotypic cell interactions. This phenomenon of cell segregation has also been described in other 3-D systems, with hepatocytes segregating to the interior of aggregates, and nonparenchymal cells lining the periphery (Landry et al. 1985; Ueno et al. 1995).

In normal liver, each hepatocyte receives nutrients and oxygen from at least one sinusoid. This blood supply is crucial to both the viability of the hepatocytes and the detoxification of blood. Currently, hepatocyte spheroids larger than about 150 μM in diameter develop necrotic centers. The incorporation of endothelial cell-lined ducts into spheroids could potentially raise the ceiling on the size constraint. In addition, many of the nonparenchymtal cells in the liver are located at or near the sinusoids, making vascularization a logical focus for further tissue engineering studies with spheroids. The stellate cell plays an important role in the process of sinusoid formation during liver

regeneration. It is therefore of particular interest to examine the interaction of HSC-T6 cells with hepatocyte spheroids *in vitro*.

Culturing cells in 3-D systems has the obvious advantage of more closely representing conditions *in vivo*, but analysis of cell behavior in such systems can be complicated. The dual dye labeling technique we employed is a simple yet powerful method to identify cell populations and observe cell movement in three dimensions. In this study, the HSC-T6 cells invaded the spheroids and penetrated a few hepatocyte layers before retracting back to the periphery of the spheroid. Similar results have been observed between hepatocytes and another activated stellate cell line, CFSC-2G. Under co-culture conditions, these stellate cells were observed extending processes between hepatocytes that later retracted to leave sinusoid-like spaces between the cells (Rojkind et al. 1995). It is unclear why the HSC-T6 cells reemerged at the surface after invading the hepatocyte spheroid, but the exact conditions that occur during liver regeneration are not reproduced in our system. For example, the hepatocytes used in these studies may have significant differences from the newly divided cells *in vivo*, important signaling factors released during liver regeneration may not be present, and other liver cell types are absent. Another factor to consider is that the behavior of the cell line may not closely mirror the behavior of stellate cells *in vivo*. Finally, the possibility exists that repeated scanning by the laser interrupted cell function even though the power was kept to a minimum and scanning occurred only once per hour.

Since spheroid formation and structure have already been well characterized, this system provides a sturdy foundation for co-culture studies. A long-term goal of these investigations is to incorporate nonparenchymal cell types into spheroids efficiently and systematically. Other researchers have explored the possibility of constructing liver organoids on three-dimensional polymer scaffolds comprised of 'vessels' seeded with hepatocytes and nonparenchymal cells (Griffith et al. 1997; Kim et al. 1998). Results indicate a reorganization of the cell types and increased activity when culture medium was perfused through the channels. The advantage of mimicking liver regeneration using hepatocyte spheroids and stellate cells is that endothelial cell lined channels could potentially be constructed in a manner and scale similar to natural events without the necessity of scaffolding, patterning or complicated culture procedures.

Acknowledgements

The HSC-T6 cells were a gift from Dr. Scott Friedman, Mount Sinai School of Medicine, New York, NY. The technical assistance of Eric Tsai, Kristine Groehler, Diane Tobolt, and Josh Wilhelm is greatly appreciated. S.F.A. was supported by a National Science Foundation graduate fellowship and a biotechnology training grant from NIGMS (GMO8347). The project was supported in part by NASA (NAG8-134) and NIH (DK453). The computational support form Minnesota Supercomputing Institute is gratefully acknowledged.

References

Abu-Absi S.F., Friend J.R., Hansen L.K. and Hu W.-S. 2002. Structural polarity and functional bile canaliculi in rat hepatocyte spheroids. Exp. Cell Res. 274: 56–67.

Agius L. 1988. Metabolic interactions of parenchymal hepatocytes and dividing epithelial cells in co-culture. Biochem. J. 252: 23–28.

Ankoma-Sey V., Wang Y. and Dai Z. 2000. Hypoxic stimulation of vascular endothelial growth factor expression in activated rat hepatic stellate cells. Hepatology 31: 141–148.

Asano K., Koide N. and Tsuji T. 1989. Ultrastructure of multicellular spheroids formed in the primary culture of adult rat hepatocytes. J. Clin. Electron Microsc. 22: 243–252.

Balis U.J., Behnia K., Dwarakanath B. and Bhatia S.N. 1999. Oxygen Consumption Characteristics of Porcine Hepatocytes. Metab. Eng. 1: 49–62.

Begue J.M., Guguen-Guillouzo C., Pasdeloup N. and Guillouzo A. 1984. Prolonged maintenance of active cytochrome P-450 in adult rat hepatocytes co-cultured with another liver cell type. Hepatology 4: 839–842.

Bhandari R., Riccalton L., Lewis A., Fry J., Hammond A., Tendler S. and Shakesheff K. 2001. Liver tissue engineering: a role for co-culture systems in modifying hepatocyte function and viability. Tissue Eng 7: 345–357.

Bhatia S.N., Balis U.J., Yarmush M.L. and Toner M. 1998. Probing heterotypic cell interactions: hepatocyte function in microfabricated co-cultures. J. Biomat. Sci. Polym. Edition 9: 1137–1160.

Chaney A. and Marback E. 1962. Modified reagents for determination of urea and ammonia. Clin. Chem. 8: 130–132.

Donato M.T., Castell J.V. and Gomez- Lechon M.J. 1991. Co-cultures of hepatocytes with epithelial-like cell lines: expression of drug-biotransformation activities by hepatocytes. Cell Biol. Toxicol. 7: 1–14.

Fawcett J. and Scott J. 1960. A rapid and precise method for the determination of urea. J. Clin. Pathol. 13: 156–160.

Friedman S.L. 1996. Hepatic stellate cells. Prog. Liver Dis. 14: 101–130.

Greenwel P., Rubin J. , Schwartz M., Hertzberg E.L. and Rojkind M. 1993. Liver fat-storing cell clones obtained from a C.C.l4-cirrhotic rat are heterogeneous with regard to proliferation, expression of extracellular matrix components, interleukin-6, and connexin 43. Lab. Invest. 69: 210–216.

Gressner A., Lahme B. and Brenzel A. 1995. Molecular dissection of the mitogenic effect of hepatocytes on cultured hepatic stellate cells. Hepatology 22: 1507–1518.

Gressner A.M., Lotfi S., Gressner G. and Lahme B. 1992. Identification and partial characterization of a hepatocyte-derived factor promoting proliferation of cultured fat-storing cells. (parasinusoidal lipocytes). Hepatology 16: 1250–1266.

Griffith L., Wu B., Cima M., Powers M., Chaignaud B. and Vacanti J. 1997. In vitro organogenesis of liver tissue. Ann. NY. Acad. Sci. 831: 382–397.

Guguen-Guillouzo C., Clement B., Baffet G., Beaumont C., Morel-Chang E., Glaise D. and Guillouzo A. 1983. Maintenance and reversibility of active albumin secretion by adult rat hepatocytes co-cultured with another liver epithelial cell type. Exp. Cell Res. 143: 47–54.

Hansen L.K., Hsiao C.C., Friend J.R., Wu F.J., Bridge G.A., Remmel R.P., Ceira F.B. and Hu W.S. 1998. Enhanced morphology and function in hepatocyte spheroids: A model of tissue self-assembly. Tissue Eng. 4: 65–74.

Hsiao C.C., Friend J.R., Wu F.J., Ko W.J., Remmel R.P. and Hu W.S. 1999. Receding cytochrome P450 activity in disassembling hepatocyte spheroids. Tissue Eng. 5: 207–221.

Imaoka S., Enomoto K., Oda Y., Asada A., Fujimori M., Shimada T., Fujita S., Guengerich F.P. and Funae Y. 1990. Lidocaine metabolism by human cytochrome P-450s purified from hepatic microsomes: comparison of those with rat hepatic cytochrome P-450s. J. Pharmacol. Exp. Ther. 255: 1385–1391.

Kim S., Utsunomiya H., Koski J., Wu B., Cima M., Sohn J., Mukai K., Griffith L. and Vacanti J. 1998. Survival and function of hepatocytes on a novel three-dimensional synthetic biodegradable polymer scaffold with an intrinsic network of channels. Ann. Surg. 228: 8–13.

Koide N., Sakaguchi K., Koide Y., Asano K., Kawaguchi M., Matsushima H., Takenami T., Shinji T., Mori M. and Tsuji T. 1990. Formation of multicellular spheroids composed of adult rat hepatocytes in dishes with positively charged surfaces and under other nonadherent environments. Exp. Cell Res. 186: 227–235.

Landry J., Bernier D., Ouellet C., Goyette R. and Marceau N. 1985. Spheroidal aggregate culture of rat liver cells: histotypic reorganization, biomatrix deposition, and maintenance of functional activities. J. Cell Biol. 101: 914–923.

Lazar A., Mann H.J., Remmel R.P., Shatford R.A., Cerra F.B. and Hu W.S. 1995. Extended liver-specific functions of porcine hepatocyte spheroids entrapped in collagen gel. In Vitro Cell. Dev. Biol–Anim. 31: 40–346.

Maher J.J. and Tzagarakis C. 1994. Partial cloning of the M. subunit of laminin from adult rat lipocytes: expression of the M. subunit by cells isolated from normal and injured liver. Hepatology 19: 764–770.

Majno G. 1979. The story of the myofibroblasts. Am. J. Surg. Pathol. 6: 535–542.

Martinez-Hernandez A. and Amenta P.S. 1995. The extracellular matrix in hepatic regeneration. FASEB J. 9: 1401–1410.

Michalopoulos G.K., Bowen W.C., Zajac V.F., Beer-Stolz D., Watkins S., Kostrubsky V. and Strom S.C. 1999. Morphogenetic events in mixed cultures of rat hepatocytes and non-parenchymal cells maintained in biological matrices in the presence of hepatocyte growth factor and epidermal growth factor. Hepatology 29: 90–100.

Morris D.L. and Davila J.C. 1996. Analysis of rat cytochrome P450 isozyme expression using semi-quantitative reverse transcriptase-polymerase chain reaction (RT-PCR). Biochem. Pharmacol. 52: 781–792.

Okamoto M., Ishida Y., Keogh A. and Strain A. 1998. Evaluation of the function of primary human hepatocytes co-cultured with the human hepatic stellate cell (HSC) line L.I.90. Int. J. Artif. Organs 21: 353–359.

Peshwa M.V., Wu F.J., Follstad B.D., Cerra F.B. and Hu W.S. 1994. Kinetics of hepatocyte spheroid formation. Biotechnol. Prog. 10: 460–466.

Peshwa M.V., Wu F.J., Sharp H.L., Cerra F.B. and Hu W-S 1996. Mechanistics of formation and ultrastructural evaluation of hepatocyte spheroids. In Vitro Cell. Dev. Biol. 32: 197–203.

Rojkind M., Novikoff P.M., Greenwel P., Rubin J., Rojas-Valencia L., de Carvalho A.C., Stockert R., Spray D., Hertzberg E.L. and Wolkoff A.W. 1995. Characterization and functional studies on rat liver fat-storing cell line and freshly isolated hepatocyte co-culture system. Am. J. Pathol. 146: 1508–1520.

Sambrook J., Fritsch E.F. and Maniatis T. 1989. Molecular Cloning: A Laboratory Manual, 2nd ed. Cold Spring Harbor Laboratory, Cold Spring Harbor, NY.

Schirmacher P., Geerts A., Peitrangelo A., Dienes H. and Rogier C. 1992. Hepatocyte growth factor/hepatopoietin A. is expressed in fat-storing cells from rat liver but not myofibroblast-like cells derived from fat-storing cells. Hepatology 15: 5–11.

Seglen P.O. 1976. Preparation of isolated rat liver cells. Method. Cell Biol. 13: 9–83.

Senoo H., Imai K., Matano Y. and Sato M. 1998. Molecular mechanisms in the reversible regulation of morphology, proliferation and collagen metabolism in hepatic stellate cells by the three-dimensional structure of the extracellular matrix. J. Gastroenterol. Hepatol. 13: S19–32.

Tong J.Z., Bernard O. and Alvarez F. 1990. Long-term culture of rat liver cell spheroids in hormonally defined media. Exp. Cell Res. 189: 87–92.

Tzanakakis E.S., Hansen L.K. and Hu W.S. 2001. The role of actin filaments and microtubules in hepatocyte spheroid self-assembly. Cell Motil. Cytoskel. 48: 175–189.

Ueno K., Kobayashi A., Takegawa N. and Satoh T. 1995. Rapid formation of multicellular spheroids composed of Propionibacterium acnes pretreated adult rat liver cells by rotary culture and their immunological properties. Res. Commun. Mol. Pathol. Pharmacol. 90: 373–387.

Ueno K., Miyashita A., Endoh E., Takezawa T., Yamazaki M., Mori Y. and Satoh T. 1992. Formation of multicellular spheroids composed of rat hepatocytes. Res. Commun. Chem. Pathol. Pharmacol. 77: 107–120.

Vogel S., Piantedosi R., Frank J., Lalazar A., Rockey D.C., Friedman S.L. and Blaner W.S. 2000. An immortalized rat liver stellate cell line (HSC-T6): a new cell model for the study of retinoid metabolism in vitro. J. Lipid Res. 41: 882–893.

Wu F.J., Friend J.R., Hsiao C.C., Zilliox M.J., Ko W.J., Cerra F.B., Hu W.S. 1996. Efficient assembly of primary rat hepatocyte spheroids for tissue engineering applications. Biotechnol. Bioeng. 50: 404–415.

Wu F.J., Friend J.R., Remmel R.P., Cerra F.B. and Hu W.S. 1999. Enhanced cytochrome P450 lAl activity of self-assembled rat hepatocyte spheroids. Cell Transplantation 8: 233–246.

Yagi K., Yamada C., Serada M., Sumiyoshi N., Michibayashi N., Miura Y. and Mizoguchi T. 1995. Reciprocal regulation of prothrombin secretion and tyrosine aminotransferase induction in hepatocytes. Eur. J. Biochem. 227: 753–756.

Zaret K.S. 2000. Liver specification and early morphogenesis. Mech. Dev. 92: 83–88.